0022-3565/11/3392-412–420$25.00
THE JOURNAL OF PHARMACOLOGY AND EXPERIMENTAL THERAPEUTICS
JPET 339:412–420, 2011

Vol. 339, No. 2
185314/3723775
Printed in U.S.A.

Characterization of a Novel Potassium-Competitive Acid Blocker of the Gastric H,K-ATPase, 1-[5-(2-Fluorophenyl)-1-(pyridin-3-ylsulfonyl)-1*H*-pyrrol-3-yl]-*N*-methylmethanamine Monofumarate (TAK-438)

Jai Moo Shin, Nobuhiro Inatomi, Keith Munson, David Strugatsky, Elmira Tokhtaeva, Olga Vagin, and George Sachs

Department of Physiology and Medicine, David Geffen School of Medicine, University of California at Los Angeles, and VA Greater Los Angeles Healthcare System, Los Angeles, California (J.M.S., K.M., D.S., E.T., O.V., G.S.); and Pharmaceutical Research Division, Takeda Pharmaceutical Company Limited, Osaka, Japan (N.I.)

Received June 23, 2011; accepted August 8, 2011

ABSTRACT

Inhibition of the gastric H,K-ATPase by the potassium-competitive acid blocker (P-CAB) 1-[5-(2-fluorophenyl)-1-(pyridin-3-ylsulfonyl)-1*H*-pyrrol-3-yl]-*N*-methylmethanamine (TAK-438), is strictly K^+-competitive with a K_i of 10 nM at pH 7. In contrast to previous P-CABs, this structure has a point positive charge (pK_a 9.06) allowing for greater accumulation in parietal cells compared with previous P-CABs [e.g., (8-benzyloxy-2-methyl-imidazo(1,2-*a*)pyridin-3-yl)acetonitrile (SCH28080), pK_a 5.6]. The dissociation rate of the compound from the isolated ATPase is slower than other P-CABs, with the $t_{1/2}$ being 7.5 h in 20 mM KCl at pH 7. The stoichiometry of binding of TAK-438 to the H,K-ATPase is 2.2 nmol/mg in the presence of Mg-ATP, vanadate, or MgP_i. However, TAK-438 also binds enzyme at 1.3 nmol/mg in the absence of Mg^{2+}. Modeling of the H,K-ATPase to the homologous Na,K-ATPase predicts a close approach and hydrogen bonding between the positively charged *N*-methylamino group and the negatively charged Glu795 in the K^+-binding site in contrast to the planar diffuse positive charge of previous P-CABs. This probably accounts for the slow dissociation and high affinity. The model also predicts hydrogen bonding between the hydroxyl of Tyr799 and the oxygens of the sulfonyl group of TAK-438. A Tyr799Phe mutation resulted in a 3-fold increase of the dissociation rate, showing that this hydrogen bonding also contributes to the slow dissociation rate. Hence, this K^+-competitive inhibitor of the gastric H,K-ATPase should provide longer-lasting inhibition of gastric acid secretion compared with previous drugs of this class.

Introduction

Acid-related diseases, especially gastroesophageal reflux disease, still are often a challenge for treatment. The introduction and use of proton pump inhibitors (PPIs; e.g., omeprazole, lansoprazole, pantoprazole, rabeprazole, and esomeprazole), drugs targeting the gastric acid pump, improved acid control and improved healing of erosive esophagitis compared with H_2 receptor antagonists, but healing still requires 8 weeks of treatment. Furthermore, more than 25% of patients with gastroesophageal reflux disease continue to have symptoms, particularly at night (Jones and Patrikios, 2008; Gisbert et al., 2009). There is therefore room for improvement of therapy by better acid control.

PPIs are acid-activated prodrugs that require the presence of acid secretion for conversion to the active form that binds covalently to certain cysteines in the luminal domain of the gastric H,K-ATPase (Besancon et al., 1997; Shin et al., 2004). Because not all H,K-ATPases are active at any one time, and the drugs are not present at effective concentrations after a

This work was supported by Takeda Pharmaceutical Company Limited; the National Institutes of Health National Institute of Diabetes and Digestive and Kidney Diseases [Grants DK053642, DK058333, DK077149]; and a U.S. VA Merit Grant Award [I01BX001006-01].

Article, publication date, and citation information can be found at http://jpet.aspetjournals.org.

doi:10.1124/jpet.111.185314.

ABBREVIATIONS: PPI, proton pump inhibitor; P-CAB, potassium-competitive acid blocker; SCH28080, (8-benzyloxy-2-methyl-imidazo(1,2-*a*)pyridin-3-yl)acetonitrile; TAK-438, 1-[5-(2-fluorophenyl)-1-(pyridin-3-ylsulfonyl)-1*H*-pyrrol-3-yl]-*N*-methylmethanamine monofumarate; PIPES, 1,4-piperazinediethanesulfonic acid; CDTA, 1,2-cyclohexylenedinitrilotetraacetic acid; EP, phosphoenzyme; TM, transmembrane; PEG, polyethylene glycol; HEK, human embryonic kidney; PDB, Protein Data Bank; PF-03716556, *N*-(2-hydroxyethyl)-*N*,2-dimethyl-8-{[(4*R*)-5-methyl-3,4-dihydro-2*H*-chromen-4-yl]amino}imidazo[1,2-*a*]pyridine-6-carboxamide; AZD0865, 8-[(2,6-dimethylbenzyl)amino]-*N*-(2-hydroxyethyl)-2,3-dimethylimidazo[1,2-*a*]pyridine-6-carboxamide.

single administration, several doses are required to capture newly active pumps and achieve steady-state inhibition of the ATPase. To ensure the exposure of as many active pumps as possible to each dose of the PPI, it is also important to administer these drugs approximately 30 min before breakfast and also before dinner if they are given twice a day. It therefore requires approximately 3 to 5 days of oral treatment for steady-state inhibition of acid secretion. The ATPase has a half-life of approximately 50 h, and therefore approximately 25% of pumps are synthesized de novo each day. Those made at night are not exposed to the PPI whether on once- or twice-a-day regimens because of the short plasma half-life of all of the PPIs, namely, 60 to 90 min. Hence, there is continuing acid secretion, especially at night, of low volume but high acidity, resulting in continuing symptoms and damage to the esophagus or stomach. Furthermore, because acid secretion is required for the effect of PPIs, there are multiple acidic excursions after the initial oral dose. Continuous once-a-day treatment with the PPIs results in approximately 70% inhibition of maximal acid output on morning dosage and 80% on twice-a-day treatment (Katz et al., 2004; Spechler et al., 2009).

These shortcomings highlight the need for antisecretory drugs with faster onset and better inhibition then the PPIs. The potassium-competitive inhibitors of the H,K-ATPase (P-CABs), which block the access of potassium ion to its binding site on the gastric H,K-ATPase, resulting in immediate inhibition of acid secretion, are an alternative that lack the deficiencies of the PPIs. The discovery that tertiary amines were K^+-competitive inhibitors of the ATPase (Im et al., 1984) led to the elucidation of the mechanism of action of an imidazo[1,2-*a*]pyridine, (8-benzyloxy-2-methyl-imidazo(1,2-*a*)pyridine-3-yl)acetonitrile (SCH28080). SCH28080 binds to the E_2 or E_2P form of the enzyme and is a strictly K^+-competitive inhibitor (Wallmark et al., 1987; Mendlein and Sachs, 1990). This mechanism allows rapid inhibition of the pump without the need for acidity at its luminal surface because the pump is blocked in midcycle without a requirement for pump activity, thus preventing transient acidic excursions (Wilder-Smith et al., 1995). However, because inhibition is reversible, with either a relatively short plasma half-life or rapid dissociation of the drug, acid secretion rapidly returns to pretreatment levels, reducing efficacy of once-a-day dosing. After the discovery of SCH28080, many P-CABs were developed based on a similar planar core structure, but they were unsatisfactory for clinical usage either because of their short duration of action or side effects such as hepatotoxicity or inhibition of the Herg K^+ channel (Berg et al., 2008; Dent et al., 2008).

Here, we describe the properties of a new reversible inhibitor of the H,K-ATPase, 1-[5-(2-fluorophenyl)-1-(pyridin-3-yl-sulfonyl)-1*H*-pyrrol-3-yl]-*N*-methylmethanamine monofumarate (TAK-438) (Fig. 1). The aim of this study is to elucidate the mechanism of inhibition by TAK-438 and evaluate the potency of this compound. This work demonstrates that TAK-438 is a selective K^+-competitive inhibitor of the H,K-ATPase with very slow reversibility, hence a long duration of action on the H,K-ATPase. Its structure when docked to a novel homology model of the gastric H,K-ATPase based on a recent three-dimensional structure of the Na,K-ATPase explains the very slow off-rate of the inhibitor compared with the imidazopyridine class of P-CABs caused by the close approach of the charged methylamino group of TAK-438 to the K^+ site at Glu795.

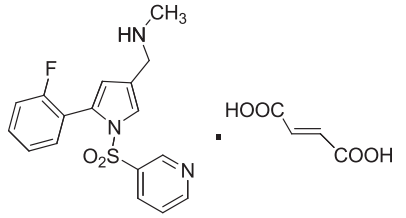

Fig. 1. Structure of TAK-438.

Materials and Methods

Hog Gastric H,K-ATPase Enzyme Preparation. Gastric H,K-ATPase was prepared from hog gastric mucosa as described previously (Sachs et al., 1976; Chang et al., 1977; Hall et al., 1990). All operations were carried out at 1 to 4°C. The crude gastric mucosal membranes were collected from the stomach and homogenized in a solution of 0.25 M sucrose, 5 mM PIPES/Tris, pH 6.8, 1 mM EDTA, and 1 mM EGTA. The homogenate was centrifuged at 20,000*g* in a Sorvall GSA rotor (Thermo Fisher Scientific, Waltham, MA) for 45 min. The pellet was discarded, and the supernatant was centrifuged at 134,000*g* in a Beckman type 35 rotor (Beckman Coulter, Fullerton, CA) for 1 h. The microsomal membrane pellet was resuspended in a solution of 0.25 M sucrose, 5 mM PIPES/Tris, pH 6.8, 1 mM EDTA, and 1 mM EGTA and was purified on a step gradient sucrose solution composed of 34% (w/v) sucrose, 5 mM PIPES/Tris, pH 6.8, 1 mM EDTA, and 1 mM EGTA overlaid by a solution composed of 7.5% Ficoll, 0.25 M sucrose, 5 mM PIPES/Tris, pH 6.8, 1 mM EDTA, and 1 mM EGTA, using a SW 28 rotor (Beckman Coulter) at 130,000*g* for 2 h. The vesicles above the 7.5% Ficoll gradient step were collected and diluted by adding 3 volumes excess of a solution of 5 mM PIPES/Tris, pH 6.8, 1 mM EDTA, and 1 mM EGTA. The suspension was centrifuged at 130,000*g* for 1 h, and the pellet was resuspended in a solution of 0.25 M sucrose and 5 mM PIPES/Tris, pH 6.8.

The membrane vesicles were more than 90% cytoplasmic side-out. Mg^{2+}-dependent activity was approximately 7 $\mu mol \cdot mg^{-1} \cdot h^{-1}$. The activity in the presence of nigericin was 95 $\mu mol\ P_i \cdot mg^{-1} \cdot h^{-1}$, and in the absence of nigericin it was only 7.6 $\mu mol \cdot mg^{-1} \cdot h^{-1}$. Thus, more than 90% of the K^+-stimulated ATPase activity depended on the addition of the K^+ ionophore, nigericin, showing that this fraction of the vesicles was K^+-impermeant with the K^+ site facing the lumen.

Measurement of Acid-Stable Phosphoenzyme Levels. Gastric vesicles (100–200 μg/ml) were incubated for 10 s at 25°C in a buffer composed of 20 mM Tris/HCl, pH 7.0, 2 mM $MgCl_2$, and [γ-^{32}P]ATP (10 μM to 0.1 mM). An aliquot (0.4 ml) was taken and added to an ice-cold stop solution (1 ml) composed of 40% trichloroacetic acid, 10 mM phosphoric acid, and 1 mM ATP. This was immediately filtered through a nitrocellulose membrane filter (HAWP Millipore filter, 0.45 μm; Millipore Corporation, Billerica, MA) prewetted with an ice-cold solution composed of 10% trichloroacetic acid and 20 mM phosphoric acid placed on top of a glass fiber filter. After washing four times with 2.5 ml of an ice-cold solution composed of 10% trichloroacetic acid and 20 mM phosphoric acid, the membrane was placed in a 20-ml scintillation vial, dimethylacetamide (0.5 ml) was added to dissolve the membrane, and 10 ml of scintillation solvent was added and counted. Nonspecific P_i binding was measured using a gastric vesicle suspension in a buffer composed of 20 mM Tris/HCl, pH 7.0, [γ-^{32}P]ATP (10 μM to 0.1 mM), and 5 mM CDTA with no Mg^{2+}, because Mg^{2+} is essential for phosphoenzyme formation. The acid-stable phosphoenzyme level was determined by subtracting the nonspecific binding obtained in the presence of CDTA-ATP from the total binding obtained in the presence of Mg-ATP.

Inhibition of ATPase Activity. ATPase activity was measured over a range of 0 to 100 mM KCl in the presence of different concentrations of TAK-438 (0–0.1 μM) and nigericin. The gastric vesicles (2–3 μg/ml) were resuspended in a buffer composed of 20 mM Tris/HCl, pH 7.0, 2 mM $MgCl_2$, 0 to 10 mM KCl, 1 μg/ml nigericin, and 0 to 0.1 μM TAK-438. Background phosphate release was measured using an enzyme suspension as described above but in the absence of $MgCl_2$. Activity was initiated by adding a final concentration of 2 mM ATP at 37°C and incubating for 30 min. Released inorganic phosphate was measured, and the ATPase activity was calculated. The results obtained for the K^+-stimulated ATPase activity were fitted to equations describing patterns of competitive, noncompetitive, and mixed inhibition by least-squares fitting using the computer program Prism 4 (GraphPad Software Inc., San Diego, CA).

The IC_{50} was determined in the presence of 10 mM KCl over a range of TAK-438 concentrations (0–0.1 μM).

Inhibition of Acridine Orange Uptake. Gastric vesicles (20 μg/ml) were suspended in a buffer composed of 3 mM Pipes/Tris, pH 7, 2 mM $MgCl_2$, 150 mM KCl, and 5 μg/ml valinomycin in the presence of 1 μM acridine orange. Acridine orange accumulation reflecting intravesicular acidification was measured using a spectrofluorimeter with the excitation wavelength at 490 nm and the emission wavelength at 530 nm. After obtaining a steady baseline, ATP was added at 2 mM using 0.1 M ATP stock solution, pH 7. After adding ATP, the enzyme acidified the lumen of the vesicles, resulting in acridine orange uptake with quenching of the fluorescence. When maximal fluorescence quenching was obtained, either SCH28080 or TAK-438 was added, and the rate of return of fluorescence was measured to estimate the relative rates of binding of the imidazopyridine and pyrrolo-pyridine.

TAK-438 Binding to the Gastric H,K-ATPase. [^{14}C]TAK-438 binding studies were carried out at 25 or 37°C. All experiments were performed at least in triplicate, and the average of the results was used for analysis. In saturation experiments to determine the binding stoichiometry of TAK-438, the gastric vesicles (0.01–0.02 mg/ml) were resuspended in a buffer composed of 20 mM Tris/HCl, pH 7.0, 2 mM $MgCl_2$, and 2 mM ATP (pH 7.0 by Tris) and in the presence of increasing concentrations of [^{14}C]TAK-438 (0.1 nM to 0.5 μM). The enzyme suspension (1 ml) was incubated at 25°C for 30 min and rapidly filtered through a nitrocellulose membrane filter (HAWP Millipore filter; 0.45 μm) prewet with a solution composed of 20 mM Tris/HCl, pH 7.0, and 10% PEG3350 that was placed on top of a glass fiber filter. The membrane was washed five times with 2.5 ml of a buffer composed of 20 mM Tris/HCl, pH 7.0, and 10% PEG3350 to remove unbound inhibitor. The membrane was placed in a 20-ml scintillation vial, dimethylacetamide (0.5 ml) was added to dissolve the membrane, 14 ml of scintillation solvent was added, and the radioactivity was counted.

Nonspecific binding of TAK-438 was determined as follows: the enzyme was preincubated with 200-fold excess of unlabeled TAK-438 over the above concentration range of [^{14}C]TAK-438 for 30 min, then treated with [^{14}C]TAK-438. After filtration and washing as described above, nonspecific binding was measured. The specific binding of [^{14}C]TAK-438 was determined by subtracting the nonspecific binding of [^{14}C]TAK-438 from the amounts of [^{14}C]TAK-438 bound to the membrane in the absence of the cold inhibitor.

To find out whether the binding is covalent or not, an aliquot of [^{14}C]TAK-438-bound enzyme was precipitated by methanol. In a typical run, an aliquot of [^{14}C]TAK-438 bound enzyme (0.1 ml) prepared as described above was treated with 1 ml of ice-cold methanol, and the mixture was incubated on ice for 30 min. The mixture was centrifuged and the protein was separated. [^{14}C]TAK-438 in the protein precipitate was counted.

In KCl competition experiments, a fixed concentration of [^{14}C]TAK-438 (10–100 nM) was incubated in the presence of varying concentrations of KCl (0.001–330 mM) at 25 or 37°C for 0.1 to 7 h as indicated in the presence and absence of nigericin (5 μg/ml). An aliquot at a given concentration of KCl was taken out at timed intervals, and the radioactivity bound to the enzyme was measured as described above.

The exchange rate of [^{14}C]TAK-438/TAK-438 was measured as follows: enzyme (0.01 mg/ml) was preincubated with 100 nM [^{14}C]TAK-438 at room temperature for 60 min. The enzyme suspension was then treated with 500-fold excess of nonlabeled TAK-438, and an aliquot was incubated at 37°C and taken out at timed intervals. The radioactivity bound to the enzyme was measured as described above.

To investigate the effects of various ligands on inhibitor binding, the gastric vesicles (0.01 mg/ml) were incubated at 37°C for 60 min in a buffer composed of 20 mM Tris/HCl, pH 7.0, and different ligands such as ± 2 mM $MgCl_2$, ± 5 (or 10) mM CDTA, ± 2 mM ATP (pH 7.0 adjusted by Tris), ± 0.2 mM vanadate, pH 7.0, and ± 5 mM P_i/Tris, pH 7.0, in the presence of 100 nM [^{14}C]TAK-438. The radioactivity bound to the enzyme was measured as described above.

Binding Stoichiometry of TAK-438 with Phosphoenzyme. To determine the stoichiometry of the inhibitor binding to the acid-stable phosphoenzyme intermediate (EP), first, EP was measured in the presence of nonlabeled TAK-438. Intact gastric vesicles were incubated at 25°C for 1 h in a buffer composed of 20 mM Tris/HCl, pH 7, 2 mM $MgCl_2$, 10 μg ml/nigericin, and 0.1 μM nonlabeled TAK-438 at a 100 μg/ml protein concentration. Using this TAK-438-bound enzyme, [γ-^{32}P]ATP was then added at a final concentration of 0.1 mM and incubated at 25°C for 10, 20, 60, and 120 s. Acid-stable EP was measured as described above. TAK-438 binding was measured as follows: intact gastric vesicles were incubated at 25°C for 1 h in a buffer composed of 20 mM Tris/HCl, pH 7, ± 2 mM $MgCl_2$, ± 10 mM CDTA, 10 μg ml/nigericin, and 0.1 μM [^{14}C]TAK-438 at a 100 μg/ml protein concentration. TAK-438 binding was measured as described above.

Dissociation Rate of TAK-438 from Wild Type and Mutants of the H,K-ATPase Expressed in HEK293 Cells. Wild type and mutants of the rabbit gastric H,K-ATPase expressed in HEK293 cells were prepared as described (Vagin et al., 2002, 2003).

Three groups of membranes containing the various forms of the H,K-ATPase were prepared as follows. In group A expressed enzyme was resuspended in a buffer composed of 50 mM Tris/HCl, pH 7, 1 mM Mg-ATP, 20 mM KCl, 2 μg/ml nigericin, and 50 nM [^{14}C]TAK-438 at a concentration of 2.5 μg/ml the H,K-ATPase. Group A was used for measuring TAK-438 dissociation by KCl. In group B expressed enzyme was resuspended in a buffer composed of 50 mM Tris/HCl, pH 7, 1 mM Mg-ATP, 2 μg/ml nigericin, and 50 nM [^{14}C]TAK-438 at a concentration of 2.5 μg/ml H,K-ATPase. This was used for measurement of the full binding of TAK-438. In group C expressed enzyme was resuspended in a buffer composed of 50 mM Tris/HCl, pH 7, 1 mM Mg-ATP, 2 μg/ml nigericin, and 50 μM cold TAK-438 at a concentration of 2.5 μg/ml H,K-ATPase. This mixture was incubated at 37°C for 30 min, and the isotope was added at a concentration of 50 nM [^{14}C]TAK-438. Group C determined the nonselective binding of TAK-438.

The enzyme suspension (1 ml) was incubated at 37°C for 0.1 to 7 h as indicated and rapidly filtered through a nitrocellulose membrane filter (HAWP Millipore filter; 0.45 μm) prewet with a solution composed of 20 mM Tris/HCl, pH 7.0, and 10% PEG3350 that was placed on top of a glass fiber filter. The nitrocellulose membrane was washed five times with 2.5 ml of a buffer composed of 20 mM Tris/HCl, pH 7.0, and 10% PEG3350 to remove unbound inhibitor. The membrane was then placed in a 20-ml scintillation vial, dimethylacetamide (0.5 ml) was added to dissolve the membrane, and 14 ml of scintillation solvent was added and counted. The quantity of TAK-438 bound to the mutant was calculated by subtracting group C from group A. Group B showed the stability of TAK-bound enzyme during the incubation period. When a significant loss of TAK binding was observed in group B, the data of group A obtained at the time of the loss were not used for analysis.

Modeling of TAK-438 Binding. A homology model of the H,K-ATPase was constructed based on the dogfish Na,K-ATPase struc-

ture, PDB 2ZXE, that contains both α and β subunits to provide a framework for predicting TAK-438 interaction with the gastric enzyme (Ogawa et al., 2009). This form of the Na,K-ATPase represents the $E_2{\cdot}2K{\cdot}P_i$ conformation to which TAK-438 binds. The peptide backbone from the PDB 2ZXE structure file was copied, and side chains were replaced with those of the H,K-ATPase based on BLASTP alignments of the rabbit H,K-ATPase α and β sequences to those of the dogfish.

Model building was performed with Insight II and Discover software (Accelrys, San Diego, CA) using the consistent valence force field. Initial side-chain dihedral angles before energy minimization were assigned to nonconserved residues based on the allowed ranges found in high-resolution structures such that no van der Waals overlap was given with neighboring conserved side chains in either the α or β subunits. Nonconserved loop replacements were made by searching a database of loop structures contained in the Searchloop module of the software for loops with the desired number of amino acids that also matched the secondary structure in the conserved regions before and after the loop. Loop replacements containing the additional, nonconserved carbohydrate sites in the H,K-ATPase β subunit (total of seven sites as opposed to three in Na,K-ATPase β subunit) were selected to allow the modified asparagines to be exposed to the exterior of the protein. After nonconserved loop and side-chain replacement, the model was energy-minimized with only conserved side chains and internal secondary structures, including disulfide bonds, held fixed. Energy minimization was carried out to an average absolute derivative of less than 0.01 kcal/mol · Å with a fixed dielectric constant of 15 and a 15-Å nonbonded cutoff.

Data Analysis and Statistics. All experiments were performed in triplicate or more, and the average of the results was used for analysis. Mean values are expressed ± S.E. of individual experiments performed.

Materials. [^{14}C]TAK-438 (specific activity, 5.17 MBq/mg) was provided by Dr. Nobuhiro Inatomi (Takeda Pharmaceutical Company Limited, Osaka, Japan). [γ-^{32}P]ATP (specific activity, 6000 Ci/mmol) was purchased from GE Healthcare (Chalfont St. Giles, Buckinghamshire, UK). [γ-^{32}P]ATP (0.25 mCi) was diluted to 2 ml in 2 mM ATP/Tris, pH 7.0, to give a radioactivity of 0.125 mCi/ml and used within 5 days. All other reagents were analytical grade or higher.

Results

H,K-ATPase Inhibition by TAK-438. In this experiment, TAK-438 inhibited the gastric H,K-ATPase with an IC_{50} of 17 nM and inhibited the enzyme K competitively. The K_i was 10 nM when measured at pH 7 (Fig. 2). A lower calculated K_i of 3 nM was reported when the K_i was measured at pH 6.5 (Hori et al., 2010). TAK-438 selectively inhibited the gastric H,K-ATPase compared with the homologous Na,K-ATPase. TAK-438 inhibits the dog and pig Na,K-ATPases with an IC_{50} of 44 and 95 μM, respectively. Given an IC_{50} of 17 nM on the gastric H,K-ATPase, this compound has a more than 1000-fold selectivity for the gastric H,K-ATPase.

To distinguish between covalent or reversible inhibition, reversibility of binding was determined. To do this, the gastric enzyme was first inhibited by TAK-438 and [^{14}C]TAK-438 binding was measured as described under *Materials and Methods*. Then, [^{14}C]TAK-438-bound enzyme was precipitated by methanol. If TAK-438 inhibited the enzyme activity via covalent binding, the protein precipitate should contain the labeled TAK-438. After methanol precipitation, only approximately 1% of TAK-438 was found in the precipitate, and ~ 99% of the labeled TAK-438 was in the supernatant after methanol precipitation. Thus TAK-438 binding to the gastric H,K-ATPase is noncovalent.

The TAK-438 binding rate was measured using inhibition of acridine orange uptake in acid-transporting H,K-ATPase vesicles and compared with SCH28080. The IC_{50} of SCH28080 is 150 nM at pH 6.5 (Wallmark et al., 1987), whereas the IC_{50} of TAK-438 is 17 nM, thus TAK-438 inhibition is approximately 10 times more potent than SCH28080. Therefore, the effect of TAK-438 at 10 nM was compared with that of SCH28080 at 100 nM. When the inhibitors were added at these concentrations, acridine orange uptake caused by the proton gradient reversed because of the inhibition of acid secretion. The slope reflects the rate of inhibition, and when calculated from the Boltzmann sigmoidal equation for inhibition of vesicle acidification was 9.6 and 42 for SCH28080 and TAK-438, respectively (Fig. 3). These data show that the rate of binding of TAK-438 is slower than SCH28080 as expected from the slow dissociation. However, given that the plateau of inhibition is reached within 30 s with SCH28080 and 200 s with TAK-438, this will not affect the efficacy of the latter on diurnal pH in vivo.

Potassium Ion Competition of TAK-438 Binding. Reversal of TAK-438 binding was investigated at various concentrations of KCl. As shown in Fig. 4, the half-time of TAK-438 dissociation by KCl was 12.5 h in the presence of 10 mM KCl, 7.5 h in the presence of 20 mM KCl, and 3 h in the presence of 300 mM KCl. The dissociation rate of TAK-438 from the isolated ATPase was slower than other P-CABs, For example, 60% of SCH28080 dissociated in the presence of 10 mM KCl in 2 min (Keeling et al., 1989). Physiologically the H,K-ATPase probably is exposed to a concentration of approximately 15 mM KCl in stimulated gastric juice, hence the in vivo dissociation rate is expected to be >7.5 h, slow enough to result in stable inhibition of acid secretion after single-dose administration.

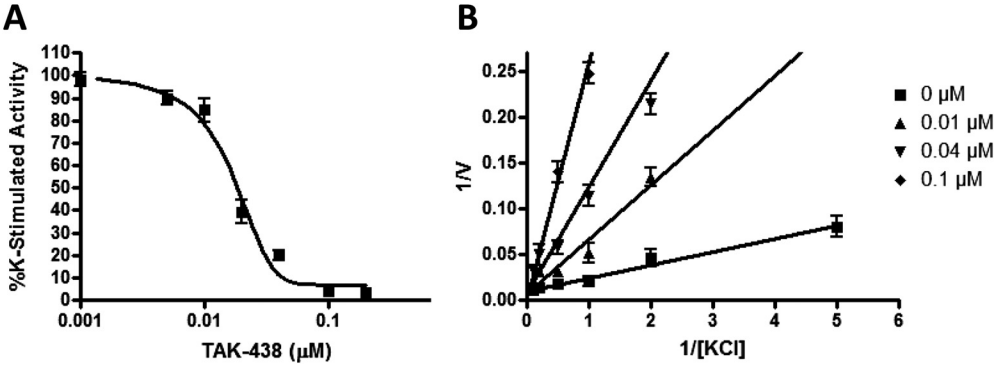

Fig. 2. Inhibition by TAK-438. A, an aliquot of the gastric H,K-ATPase enzyme suspension (3 μg/ml) was preincubated in a buffer composed of 10 mM KCl, 2 mM $MgCl_2$, ± 2 μg/ml nigericin, and 20 mM Tris/HCl, pH 7.4, for 2 h, and the enzyme activity was measured by adding 2 mM ATP for 30 min at 37°C. B, 1/V versus 1/[KCl] plot in the presence of different fixed concentrations of TAK-438. V represents the enzyme activity (μmol $P_i \cdot mg^{-1} \cdot h^{-1}$). [KCl] represents a concentration of KCl (mM). Each point represents mean ± S.E. of three experiments.

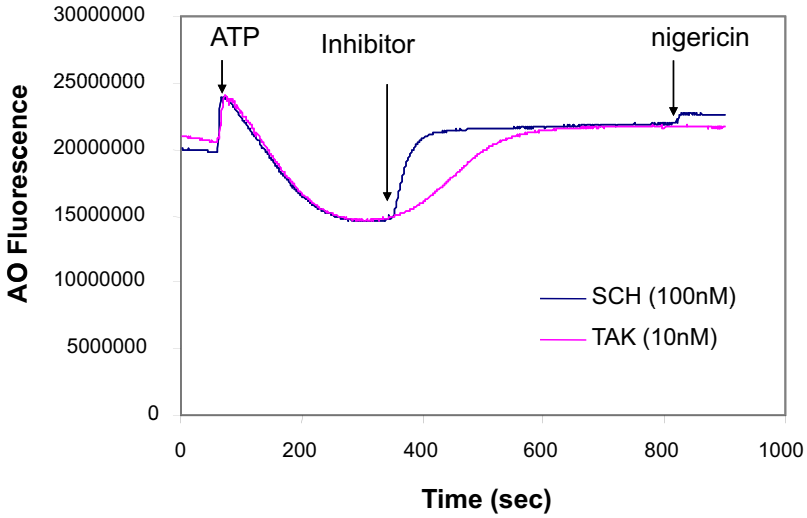

Fig. 3. The enzyme suspension (20 μg/ml) in a buffer composed of 3 mM PIPES/Tris, pH 7, 2 mM $MgCl_2$, 150 mM KCl, 5 μg/ml valinomycin, and 1 μM acridine orange (AO) was preincubated at 37°C in a cell of a spectrofluorimeter for 5 min. After 60 s, ATP (2 mM) was added to initiate acridine orange uptake. The inhibitor was added at the time as indicated by P-CAB. SCH and TAK represent SCH28080 and TAK-438, respectively.

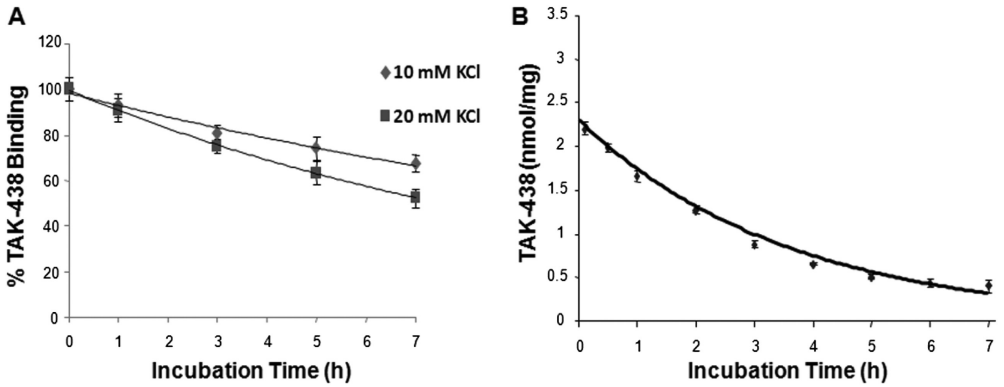

Fig. 4. Dissociation of TAK-438 binding by KCl at different incubation times. A, enzyme (10 μg/ml) was resuspended in a buffer composed of 50 mM Tris/HCl, pH 7.0, 2 mM $MgCl_2$, 2 mM ATP, and 50 nM [^{14}C]TAK-438 and incubated at room temperature (25°C) for 60 min. Under this condition, TAK-438 binds to the enzyme with full inhibition. To this enzyme suspension, KCl was added at 10 or 20 mM and incubated at 37°C. At timed intervals, an aliquot was taken to measure the binding. B, enzyme (10 μg/ml) was resuspended in a buffer composed of 50 mM Tris/HCl, pH 7.0, 2 mM $MgCl_2$, 2 mM ATP, and 100 nM [^{14}C]TAK-438 and incubated at room temperature (25°C) for 60 min. Under these conditions, TAK-438 binds to the enzyme with full inhibition. To this enzyme suspension, KCl was added up to 0.3 M final concentration and incubated at 37°C. At timed intervals, an aliquot was taken to measure the binding as described under *Materials and Methods*.

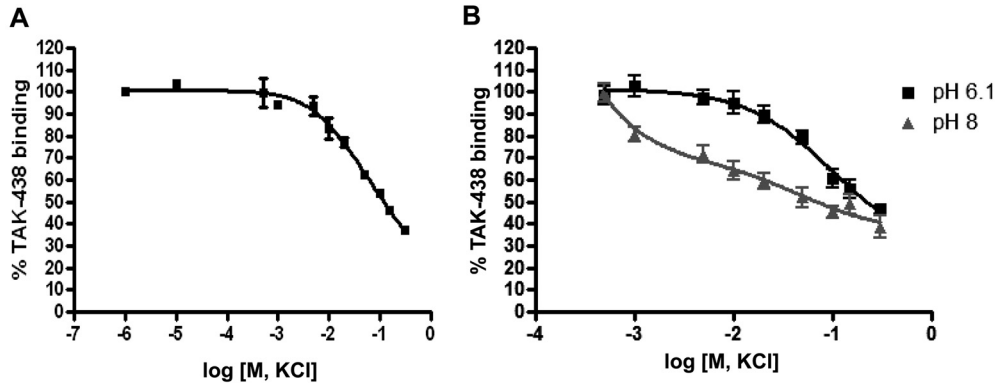

Fig. 5. Dissociation of TAK-438 binding as a function of KCl concentration and medium pH. A, enzyme (5 μg/ml) was resuspended in a buffer composed of 2 mM $MgCl_2$, 2 mM ATP, 2 μg of nigericin/ml, 50 nM [^{14}C]TAK-438, and 50 mM Tris/HCl, pH 7.0. The enzyme suspension at pH 7 was incubated at 37°C for 3 h in the presence of various concentrations of KCl. B, the enzyme suspensions at pH 6.1 and 8 were treated identically except for incubation time and temperature. These enzyme suspensions were incubated at 25°C for 2 h. TAK-binding was measured as described under *Materials and Methods*. In this experiment, TAK-438 binding measured in the absence of KCl was 2.15 nmol/mg at 50 nM TAK-438. This was taken as representing 100% binding, allowing calculation of the percentage of TAK-438 binding at given KCl concentrations.

The rate of dissociation of TAK-438 binding increased as the concentration of K ion increased. As shown in Fig. 5A, approximately half of TAK-438 binding dissociated in 150 mM KCl after 3-h incubation after 50 nM [^{14}C]TAK-438 treatment. When a higher concentration of TAK-438 was used, a higher KCl concentration was required to get the same degree of TAK-438 dissociation.

The dissociation rate was affected by medium pH. TAK-

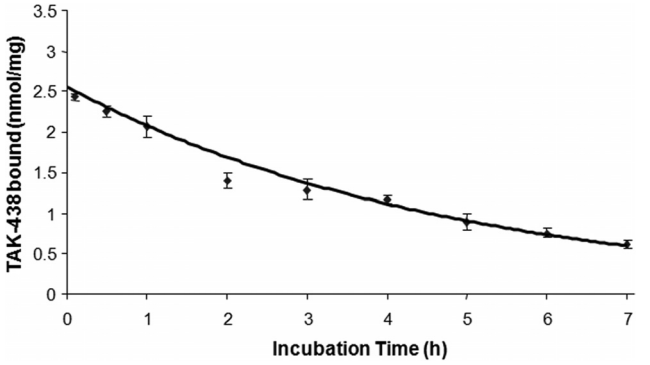

Fig. 6. Exchange of bound [^{14}C]TAK-438 by unbound unlabeled TAK-438 after different incubation times. Enzyme (10 μg/ml) was resuspended in a buffer composed of 50 mM Tris/HCl, pH 7.0, 2 mM $MgCl_2$, 2 mM ATP, and 100 nM [^{14}C]TAK-438 and incubated at room temperature (25°C) for 60 min. Under these conditions, TAK-438 binds to the enzyme with full inhibition. To this enzyme suspension, nonlabeled TAK-438 was added up to 50 μM final concentration and incubated at 37°C. At timed intervals, an aliquot was taken to measure the exchange as described under *Materials and Methods*.

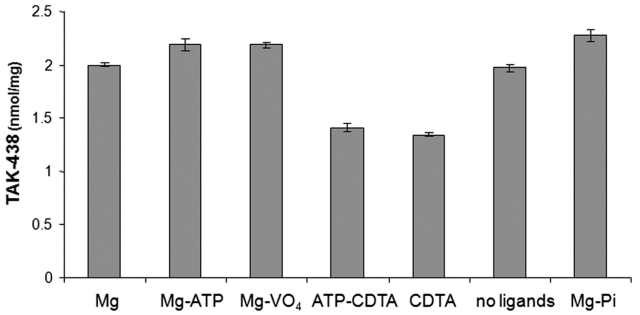

Fig. 7. Effects of various ligands on TAK-438 binding. The gastric vesicles (0.01 mg/ml) were incubated at 37°C for 60 min in a buffer composed of 50 mM Tris/HCl, pH 7.0, and different ligands such as ± 2 mM $MgCl_2$, ± 5 mM CDTA, ± 2 mM ATP, ± 0.2 mM vanadate, and ± 5 mM P_i/Tris, pH 7.0, in the presence of [^{14}C]TAK-438 (100 nM). Binding stoichiometry was determined as described under *Materials and Methods*.

438 is a basic amine with the methylamino group having a calculated pK_a of 9.06. The pK_a of the pyridine is probably very low (calculated pK_a = 0.38) because of electron withdrawal by the sulfonyl substituent and unlikely to contribute to the pH dependence of binding. Thus, in acidic media, the effect of TAK-438 on the enzyme is somewhat less sensitive to KCl at pH 6.1 than that at pH 8 because of increased protonation of the methylamino group and therefore stronger binding (Fig. 5B). This implies that the protonated form of TAK-438 has a higher affinity for its binding site on the enzyme, consistent with the model described below.

Displacement of TAK-438 Binding. The reversibility of TAK-438 bound to the enzyme was measured by displacement of isotope-labeled TAK-438 by unlabeled TAK-438. TAK-438 binding to the enzyme was carried out using radiolabeled TAK-438 as described under *Materials and Methods* and then nonlabeled TAK-438 was added at 500-fold higher concentration compared with labeled TAK-438, and an aliquot was taken out at timed intervals to measure the isotope binding. Half of the labeled TAK-438 was exchanged after 3.5 h of incubation with 500-fold excess of nonlabeled TAK-438 (Fig. 6). This prolonged dwell time is similar to that seen with KCl-dependent reversal.

This slow dissociation of enzyme-bound TAK-438 both with extremely high concentrations of KCl or nonlabeled TAK-438 shows that TAK-438 binding is remarkably stable compared with the rapid reversal of the effects of the imidazopyridine class of compound.

Stoichiometry and ligand Effects on TAK-438 Binding. TAK-438 binding studies were carried out at 25 or 37°C. Because TAK-438 binding was slow compared with other P-CABs such as SCH28080 or BYK compounds, we incubated TAK-438 for longer times. TAK-438 binding stoichiometry was determined using [^{14}C]TAK-438 (0.1 μM) in the presence of various ligands (Fig. 7). The stoichiometry of binding of TAK-438 to the H,K-ATPase was 2.2 nmol/mg in the presence of Mg-ATP, magnesium vanadate, or MgP_i. Given the purity of G1 as 85%, TAK-438 binding to the H,K-ATPase was same as other P-CABs, namely approximately 2.6 nmol/mg (Shin et al., 2005) with a 1:1 stoichiometry with respect to EP. TAK-438 binds to the enzyme with reduction of stoichiometry to approximately 1.3 to 1.4 nmol/mg in the presence of the magnesium ion chelator (CDTA), i.e., in the absence of Mg^{2+}. This result is different from other P-CABs such as SCH28080 that do not bind in the absence of magnesium ion. Hence, TAK-438 binding does not require the Mg^{2+}-induced conformational changes of the H,K-ATPase compared with other P-CABs. Because the pump is a dimeric oligomer (Shin et al., 2005), it seems possible that the resting conformation in the absence of Mg^{2+} allows docking of TAK-438 because of the close approach of the protonated methylamino group in contrast to the more distant binding of the imidazopyridines.

Dissociation Rate of TAK-438 from Mutants of the H,K-ATPase. The wild-type rabbit H,K-ATPase expressed in HEK293 cells gave a similar stoichiometry of TAK-438 binding to the pig H,K-ATPase. Dissociation of TAK-438 binding from the rabbit H,K-ATPase expressed in HEK293 cells was a little faster than that from the pig H,K-ATPase prepared from the stomach. The $t_{1/2}$ of dissociation of TAK-438 binding was 4.7 h. The mutants M334A and M334I had an unchanged $t_{1/2}$ of binding at 4.1 and 4.9 h, respectively. However the mutant Y799F had a $t_{1/2}$ of 1.5 h (Table 1), demonstrating a minor role of the -OH group of the tyrosine at position 799 compared with hydrogen bonding with the methylamino group of TAK-438. The major determinant of the slow dissociation rate is probably the hydrogen-bonding interaction between the K^+ site at Glu795 and the methylamino group on TAK-438.

Molecular Modeling of the Gastric H,K-ATPase Based on the Crystal Structure of the Dogfish Na,K-ATPase. The gastric H,K-ATPase belongs to the class of P_2-type membrane ATPases. Two members of the class have been crystallized and their structures determined, the srCa-ATPase in several on its conformations and the Na,K-ATPase

TABLE 1

TAK-438 dissociation of the mutants expressed in HEK293 cells

Wild type and mutants of the rabbit gastric H,K-ATPase expressed in HEK293 cells were prepared at a concentration of 2.5 μg/ml the H,K-ATPase. Each mutant was incubated with 50 nM [^{14}C]TAK-438, and the dissociation of TAK-438 was measured as described under *Materials and Methods*.

Mutant	Half-Time of TAK-438 Dissociation
	h
Wild type	4.7
M334A	4.1
M334I	4.9
Y799F	1.5

in the conformation that has the K^+ counter ion occluded (E_2·2K·P_i). This state of the gastric H,K-ATPase is generated after K^+ binding to the E_2-P conformation, which also binds the K^+-competitive inhibitors. Previously, the binding site location was identified with the aid of a large array of point mutations of the H,K-ATPase whose effects on activity and inhibitor affinity were evaluated. The results were used to assign the placement of the inhibitors in the models for energy minimization (Vagin et al., 2002; Munson et al., 2005, 2007). The predicted orientation of SCH28080 was further restricted by biochemical results, which included photoaffinity labeling of the TM1/TM2 pair of membrane helices with a derivative modified with azide in the *para* position of the phenyl ring and by pharmacological studies that defined the active conformation for this inhibitor (Munson et al., 1991). The binding site was localized to a cavity next to the TM5/TM6 loop within the membrane domain. This assumption is now supported in the recent crystal structure of the Na,K-ATPase, PDB 2ZXE. which shows a vestibule in the same location that provides the site of ouabain binding in the Na,K-ATPase and for omeprazole binding to Cys813 in the H,K-ATPase. This demonstrates the substantial accuracy of the homology modeling approach. The H,K- and Na,K-ATPases both possess a β subunit. We therefore generated a homology model of the rabbit H,K-ATPase to include both the α and β subunits from the Na,K-ATPase PDB 2ZXE structure (Ogawa et al., 2009). The high homology between the Na,K- and H,K-ATPases is expected to give this model improved accuracy over the one based on the srCa-ATPase. SCH28080 and TAK-438 were each docked to the new model in the vestibular space next to TM5/TM6 and then energy-minimized. The vertical view of the H,K-ATPase model with TAK-438 bound (Fig. 8) shows the arrangement of the nucleotide binding (N), phosphorylation (P), actuator (A), membrane associated, and β subunit domains in the E_2 configuration. The inhibitor gains access to its binding site from the lumen through a wide entry space bounded by the TM1/TM2 and TM5/TM6 loops and the extracytoplasmic ends of TM4, TM8, and TM9. There is no apparent contribution from the β subunit for either entry or binding. After entry of the inhibitor, the space closes and the inhibitor is trapped in the vestibule. The location of the positively charged *N*-methylamino side chain of TAK-438 is within 2.4 Å of Glu795, producing strong hydrogen bonding and charge interaction with the K^+ site at Glu795 in contrast to SCH28080 and other P-CABs. Presumably Mg^{2+} is required to generate a form of the luminal vestibule that is essential for binding of the imidazopyridines but not the pyrrolo-pyridines to explain binding of the latter in the absence of Mg^{2+}. Another difference in predicted binding of TAK-438 to the vestibule in the H,K-ATPase is the suggested hydrogen bonding between Tyr799 and the sulfone of the inhibitor as shown in Fig. 9 where we compare the predicted binding of SCH28080 and TAK-438 on the Na,K-ATPase-based model of the H,K-ATPase, showing H bonding between the sulfone and Tyr799.

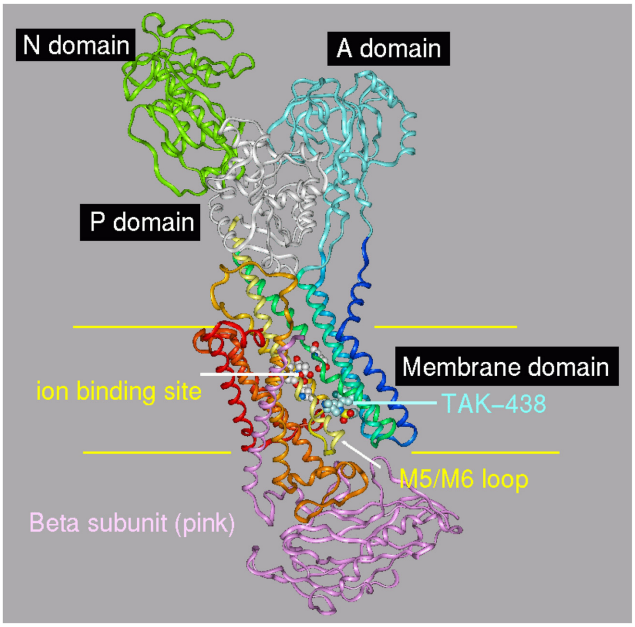

Fig. 8. Ribbon representation of the H,K-ATPase model based on the crystallographic structure of the Na,K-ATPase, PDB 2ZXE. The major domains are noted, and the position of the membrane is indicated with yellow lines: TM1, dark blue; TM2, cyan; TM3, light green; TM4, green-blue; TM5, light yellow; TM6, dark yellow; TM7, light brown; TM8, dark brown; TM9, light red; TM10, dark red. This color scheme is maintained in all figures. The position of the ion binding site is close to the middle of the membrane (ball and stick). The inhibitor, TAK-438 (space filling in light blue), binds ~10 Å from the ion binding sight in a cavity bounded by TM1, TM2, TM4, and the TM5-TM6 loop. The N-terminal 27 residues of the β subunit (pink ribbon) are not present in the Na,K-ATPase structure PDB 2ZXE and therefore are not in the HKzxe model.

Discussion

Rapid and complete inhibition of the gastric H,K-ATPase is the goal for controlling acid secretion in the stomach. Here, we have described properties of TAK-438 that make it superior to all other known inhibitors of the gastric acid pump. In vitro assays using isolated hog H,K-ATPase gave an IC_{50} of 17 nM. Thus, TAK-438 inhibits the gastric acid pump more effectively than other P-CAB inhibitors. For example, imidazopyridine types of P-CABs such as (8-[(2,6-dimethylbenzyl)amino]-*N*-(2-hydroxyethyl)-2,3-dimethylimidazo[1,2-*a*]pyridine-6-carboxamide (AZD0865), revaprazan, and *N*-(2-hydroxyethyl)-*N*,2-dimethyl-8-{[(4*R*)-5-methyl-3,4-dihydro-2*H*-chromen-4-yl]amino}imidazo[1,2-*a*]pyridine-6-carboxamide (PF-03716556) have an IC_{50} of approximately 1 μM (Gedda et al., 2007; Mori et al., 2009). Until TAK-438 was discovered, the best inhibition by a P-CAB was achieved by an imidazo-naphthyridine type of P-CAB, soraprazan, which has an IC_{50} of 100 nM (Shin et al., 2005; Simon et al., 2007). TAK-438 is at least five times more potent than soraprazan. Given that omeprazole and many other PPIs also have IC_{50} values of approximately 1 μM, TAK-438 is the most potent antisecretory agent among all of these inhibitors, PPIs, and P-CABs, based on its affinity.

The effectiveness of TAK-438 inhibition is caused by binding of the inhibitor close to the K ion binding site located in the luminal domain of the H,K-ATPase. TAK-438 competes with K^+ and the inhibition of TAK-438 is reversible. TAK-438 binding is remarkably stable, with very slow dissociation in the presence of even very high K^+ concentrations. A possible explanation is given by the homology model, which suggests that TAK-438 is bound closer to the K^+ binding site of the enzyme at Glu795, enabling strong hydrogen bonding with the carboxylates of the ion binding site.

The TAK-438 binding stoichiometry was 2.2 to 2.3 nmol/mg in the presence of Mg-ATP and a 1:1 ratio of stoichiometry of

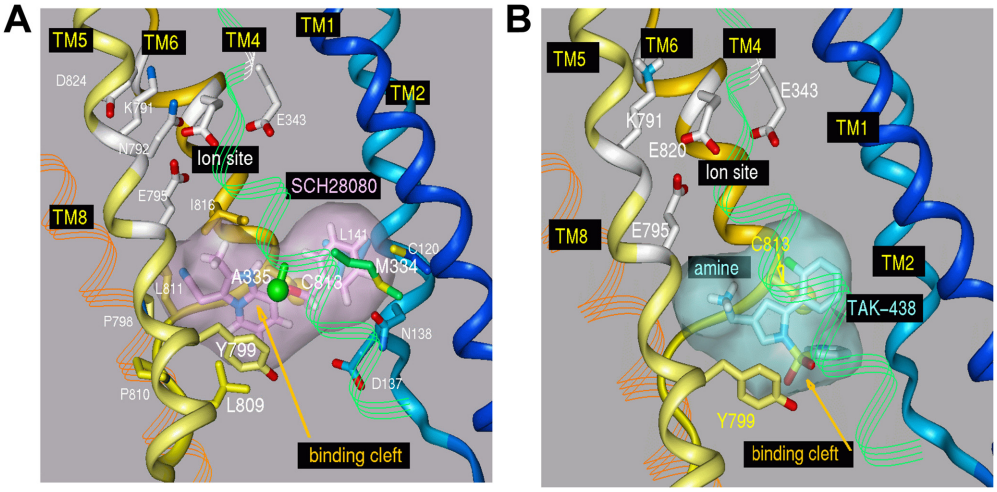

Fig. 9. A, SCH28080 binding to the H,K-ATPase model based on PDB 2ZXE. Binding is in the space between Ala335 and Cys813 (green and yellow spheres, respectively). TM1 and TM2 helices (light blue and blue, respectively) enclose the site to the right providing interaction between the inhibitor and Cys120, Asn138, Leu141, and Asp137 (stick). There is also a closer approach by the inhibitor to Pro798 (TM8) and Met334 (TM4) than in previously published models. The binding site is stabilized from below by aromatic interactions between Tyr799 and Phe332 (below Ala335 in TM4; not shown for clarity). B, binding of TAK-438 to the H,K-ATPase. The inhibitor is predicted to bind in the same cleft as SCH28080. Hydrogen bonding between Tyr799 and the sulfonyl oxygens of the inhibitor and the proximity of its amino group to the ion binding site are predicted to contribute to the slow off rate for TAK-438.

P-CAB binding relative to the phosphoenzyme. Like other P-CABs, one molecule of TAK-438 was enough to inhibit one dimeric oligomeric form of the gastric enzyme (Shin et al., 2005). Saturation of binding by TAK-438 was achieved in the presence of Mg-ATP, MgP_i, or magnesium vanadate. Even though TAK-438 binding was maximal in the presence of Mg-ATP, MgP_i, or magnesium vanadate, approximately 50% of TAK-438 bound to the enzyme in the presence of CDTA, a chelator of magnesium ion, as shown in Fig. 6. The binding rate of TAK-438 in the absence of magnesium ion was slow (data not shown), compared with the binding rate in the presence of magnesium ion. However, this TAK-438 binding in the absence of Mg^{2+} ion differs from other P-CABs such as SCH28080, AZD0865, revaprazan, and soraprazan, because these P-CABs do not bind to the gastric enzyme at all in the absence of magnesium (Mendlein and Sachs, 1990; Shin et al., 2005; Simon et al., 2007). This implies that the details of binding of TAK-438 differ from these other P-CABs, perhaps because of its hydrogen-bonding ability allowing binding even in the absence of Mg^{2+}. This result might be explained by the possible dimeric form of the H,K-ATPase oligomer (Shin et al., 2005) where TAK-438 may be able to bind to half of the dimer in the absence of magnesium.

Molecular modeling of TAK-438 binding in comparison with SCH28080 binding explains the differences in kinetic properties of the two inhibitors. SCH28080 binding in the model occurs in a cleft between Cys813 and Ala335, which is bounded on one end by Pro798 and Leu809-Leu811 and on the other by Met334, Leu141, Cys120, Asp137, and Asn138 (Fig. 9A). Tyr799 and Phe332 contact the inhibitor on the luminal side. Genetic engineering has shown that mutation of these residues reduces SCH28080 binding (Asano et al., 2004). The PDB 2ZXE Na,K-ATPase structure, however, has only ~6 Å between the positions equivalent to Cys813 and Ala335. This is at least 3 Å too narrow to accommodate SCH28080 and explains the competitive nature of this inhibitor where binding cannot occur to the K^+ occluded conformation. Docking and energy minimization of SCH28080 in this narrow space expanded the cavity with displacement of the TM4 and TM1 helices. The same type of expansion is observed when ouabain diffuses into crystals of the Na,K-ATPase, giving low affinity binding (Ogawa et al., 2009). Furthermore, the orientation of these helices with respect to the TM5/TM6 loop is different in the various known conformational states of the srCa-ATPase, demonstrating their positional flexibility. The closer proximity of the TM1/TM2 segments in the new model predicts that the side chains of Cys120, Asp137, Asn138, and Leu141 enclose the phenyl ring of SCH28080. This accounts for the photo-activated insertion of the *para*-azido derivative into this region of the protein (Munson et al., 1991). It is important to note that the distance of SCH28080 from the K binding site does not allow H bonding between the inhibitor and the pump.

The modeled binding (Fig. 9B) of TAK-438 (surfaced stick in blue in Fig. 9B) to the H,K-ATPase shares many similarities with SCH28080 but also important differences. Docking is again in a cleft between Ala335 and Cys813 and is enclosed on one end by the TM5TM6 loop (Pro798 and Leu809 to Leu811) and TM1 and TM2 with residues Leu141, Cys120, Asp137, and Asn138 (some residues not shown for clarity in Fig. 9; compare Fig. 8). Unlike SCH28080, however, TAK-438 shows additional interactions that contribute to the extremely slow off rate of this inhibitor. Most important is the proximity of its positively charged *N*-methylamino group of TAK-438 to the negatively charged group of side chains in the ion binding site, especially Glu795, that cannot happen with the imidazopyridines. A less important interaction is the hydrogen bonding between the hydroxyl of Tyr799 and the oxygens of the sulfonyl group of TAK-438. The faster dissociation of TAK-438 from the T799F mutant of the H,K-ATPase supports this detail of the model.

In vivo in the rat TAK-438 exerts a more potent and longer-lasting antisecretory effect than previous PCABs and even PPIs, because of various factors. One is the greater accumulation of TAK-438 caused by its higher pK_a, resulting in slow clearance from gastric tissue (Hori et al., 2011; Matsukawa et

al., 2011) lasting for the full 24-h time span after a single dose in the rat. Second is the slow dissociation of TAK-438 once bound, giving a long duration of action. An additional benefit of acid inhibition by this compound is that it is independent of acid secretion; hence it is mealtime-independent again in contrast to PPIs. The slow dissociation rate of TAK-438, as discussed above, is accompanied by a slow on rate, and this kinetic property helps explain the effectiveness of acid secretory inhibition by this novel K^+ competitive antagonist.

Acknowledgments

We thank Drs. Jeffry Kraut and David Scott for helpful suggestions and Dr. Mark Holoboski for the pK_a calculations.

Authorship Contributions

Participated in research design: Shin and Sachs.

Conducted experiments: Shin, Munson, Strugatsky, Tokhtaeva, and Vagin.

Contributed new reagents or analytic tools: Shin and Inatomi.

Performed data analysis: Shin and Munson.

Wrote or contributed to the writing of the manuscript: Shin, Inatomi, Munson, and Sachs.

References

Asano S, Yoshida A, Yashiro H, Kobayashi Y, Morisato A, Ogawa H, Takeguchi N, and Morii M (2004) The cavity structure for docking the K(+)-competitive inhibitors in the gastric proton pump. *J Biol Chem* **279:**13968–13975.

Berg AL, Böttcher G, Andersson K, Carlsson E, Lindström AK, Huby R, Håkansson H, Skånberg-Wilhelmsson I, and Hellmold H (2008) Early stellate cell activation and veno-occlusive-disease (VOD)-like hepatotoxicity in dogs treated with AR-H047108, an imidazopyridine proton pump inhibitor. *Toxicol Pathol* **36:**727–737.

Besancon M, Simon A, Sachs G, and Shin JM (1997) Sites of reaction of the gastric H,K-ATPase with extracytoplasmic thiol reagents. *J Biol Chem* **272:**22438–22446.

Chang H, Saccomani G, Rabon E, Schackmann R, and Sachs G (1977) Proton transport by gastric membrane vesicles. *Biochim Biophys Acta* **464:**313–327.

Dent J, Kahrilas PJ, Hatlebakk J, Vakil N, Denison H, Franzén S, and Lundborg P (2008) A randomized, comparative trial of a potassium-competitive acid blocker (AZD0865) and esomeprazole for the treatment of patients with nonerosive reflux disease. *Am J Gastroenterol* **103:**20–26.

Gedda K, Briving C, Svensson K, Maxvall I, and Andersson K (2007) Mechanism of action of AZD0865, a K+-competitive inhibitor of gastric H+,K+-ATPase. *Biochem Pharmacol* **73:**198–205.

Gisbert JP, Cooper A, Karagiannis D, Hatlebakk J, Agréus L, Jablonowski H, and Tafalla M (2009) Management of gastro-oesophageal reflux disease in primary care: a European observational study. *Curr Med Res Opin* **25:**2777–2784.

Hall K, Perez G, Anderson D, Gutierrez C, Munson K, Hersey SJ, Kaplan JH, and Sachs G (1990) Location of the carbohydrates present in the HK-ATPase vesicles isolated from hog gastric mucosa. *Biochemistry* **29:**701–706.

Hori Y, Imanishi A, Matsukawa J, Tsukimi Y, Nishida H, Arikawa Y, Hirase K, Kajino M, and Inatomi N (2010) 1-[5-(2-Fluorophenyl)-1-(pyridin-3-ylsulfonyl)-1*H*-pyrrol-3-yl]-*N*-methylmet hanamine monofumarate (TAK-438), a novel and potent potassium-competitive acid blocker for the treatment of acid-related diseases. *J Pharmacol Exp Ther* **335:**231–238.

Hori Y, Matsukawa J, Takeuchi T, Nishida H, Kajino M, and Inatomi N (2011) A study comparing the antisecretory effect of TAK-438, a novel potassium-competitive acid blocker, with lansoprazole in animals. *J Pharmacol Exp Ther* **337:**797–804.

Im WB, Blakeman DP, Mendlein J, and Sachs G (1984) Inhibition of (H+ + K+)-ATPase and H+ accumulation in hog gastric membranes by trifluoperazine, verapamil and 8-(*N*,*N*-diethylamino)octyl-3,4,5-trimethoxybenzoate. *Biochim Biophys Acta* **770:**65–72.

Jones R and Patrikios T (2008) The effectiveness of esomeprazole 40 mg in patients with persistent symptoms of gastro-oesophageal reflux disease following treatment with a full dose proton pump inhibitor. *Int J Clin Pract* **62:**1844–1850.

Katz PO, Castell DO, Chen Y, Andersson T, and Sostek MB (2004) Intragastric acid suppression and pharmacokinetics of twice-daily esomeprazole: a randomized, three-way crossover study. *Aliment Pharmacol Ther* **20:**399–406.

Keeling DJ, Taylor AG, and Schudt C (1989) The binding of a K+ competitive ligand, 2-methyl,8-(phenylmethoxy)imidazo(1,2-a)pyridine 3-acetonitrile, to the gastric (H+ + K+)-ATPase. *J Biol Chem* **264:**5545–5551.

Matsukawa J, Hori Y, Nishida H, Kajino M, and Inatomi N (2011) A comparative study on the modes of action of TAK-438, a novel potassium-competitive acid blocker, and lansoprazole in primary cultured rabbit gastric glands. *Biochem Pharmacol* **81:**1145–1151.

Mendlein J and Sachs G (1990) Interaction of a K(+)-competitive inhibitor, a substituted imidazo[1,2a] pyridine, with the phospho- and dephosphoenzyme forms of H+, K(+)-ATPase. *J Biol Chem* **265:**5030–5036.

Mori H, Tonai-Kachi H, Ochi Y, Taniguchi Y, Ohshiro H, Takahashi N, Aihara T, Hirao A, Kato T, Sakakibara M, et al. (2009) *N*-(2-hydroxyethyl)-*N*,2-dimethyl-8-{[(4*R*)-5-methyl-3,4-dihydro-2*H*-chromen-4-yl]amino}imidazo[1,2-a]pyridine-6-carboxamide (PF-03716556), a novel, potent, and selective acid pump antagonist for the treatment of gastroesophageal reflux disease. *J Pharmacol Exp Ther* **328:**671–679.

Munson K, Garcia R, and Sachs G (2005) Inhibitor and ion binding sites on the gastric H,K-ATPase. *Biochemistry* **44:**5267–5284.

Munson K, Law RJ, and Sachs G (2007) Analysis of the gastric H,K ATPase for ion pathways and inhibitor binding sites. *Biochemistry* **46:**5398–5417.

Munson KB, Gutierrez C, Balaji VN, Ramnarayan K, and Sachs G (1991) Identification of an extracytoplasmic region of H+,K(+)-ATPase labeled by a K(+)-competitive photoaffinity inhibitor. *J Biol Chem* **266:**18976–18988.

Ogawa H, Shinoda T, Cornelius F, and Toyoshima C (2009) Crystal structure of the sodium-potassium pump (Na+,K+-ATPase) with bound potassium and ouabain. *Proc Natl Acad Sci U S A* **106:**13742–13747.

Sachs G, Chang HH, Rabon E, Schackman R, Lewin M, and Saccomani G (1976) A nonelectrogenic H+ pump in plasma membranes of hog stomach. *J Biol Chem* **251:**7690–7698.

Shin JM, Cho YM, and Sachs G (2004) Chemistry of covalent inhibition of the gastric (H+, K+)-ATPase by proton pump inhibitors. *J Am Chem Soc* **126:**7800–7811.

Shin JM, Grundler G, Senn-Bilfinger J, Simon WA, and Sachs G (2005) Functional consequences of the oligomeric form of the membrane-bound gastric H,K-ATPase. *Biochemistry* **44:**16321–16332.

Simon WA, Herrmann M, Klein T, Shin JM, Huber R, Senn-Bilfinger J, and Postius S (2007) Soraprazan: setting new standards in inhibition of gastric acid secretion. *J Pharmacol Exp Ther* **321:**866–874.

Spechler SJ, Barker PN, and Silberg DG (2009) Clinical trial: intragastric acid control in patients who have Barrett's esophagus: comparison of once- and twice-daily regimens of esomeprazole and lansoprazole. *Aliment Pharmacol Ther* **30:**138–145.

Vagin O, Denevich S, Munson K, and Sachs G (2002) SCH28080, a K+-competitive inhibitor of the gastric H,K-ATPase, binds near the M5–6 luminal loop, preventing K+ access to the ion binding domain. *Biochemistry* **41:**12755–12762.

Vagin O, Munson K, Denevich S, and Sachs G (2003) Inhibition kinetics of the gastric H,K-ATPase by K-competitive inhibitor SCH28080 as a tool for investigating the luminal ion pathway. *Ann NY Acad Sci* **986:**111–115.

Wallmark B, Briving C, Fryklund J, Munson K, Jackson R, Mendlein J, Rabon E, and Sachs G (1987) Inhibition of gastric H+,K+-ATPase and acid secretion by SCH 28080, a substituted pyridyl(1,2a)imidazole. *J Biol Chem* **262:**2077–2084.

Wilder-Smith CH, Bettschen HU, and Merki HS (1995) Individual and group dose-responses to intravenous omeprazole in the first 24 h: pH-feedback-controlled and fixed-dose infusions. *Br J Clin Pharmacol* **39:**15–23.

Address correspondence to: Dr. Jai Moo Shin, Membrane Biology Laboratory, VA Greater Los Angeles Healthcare System, 11301 Wilshire Blvd., Bldg. 113, Rm 324, Los Angeles, CA 90073. E-mail: jaishin@ucla.edu